

Use of Image Warping Techniques to Correct and Interpret Infrared Sensor Data for Navigation *

L. Wyard-Scott

Q.-H. M. Meng †

ART (Advanced Robotics & Teleoperation) Lab
Department of Electrical Engineering
University of Alberta
Edmonton, AB, T6G 2G7, CANADA
E-mail: wyard@ee.ualberta.ca, mmeng@ee.ualberta.ca

Abstract—

This paper proposes a method in which sensor fusion techniques coupled with image warping algorithms are used to interpret the signals from two infrared (IR) sensors to relate measures of distance and orientation relative to an obstacle. Development of the algorithm involves modelling of the sensor responses using a set of polynomials. The models are used to develop a ‘contour’ model which yields a closed-form expression for warping of the sensor levels into a distance-angle plane. The bounds of operation of the algorithm are dictated by the accuracy of the modelling process.

I. INTRODUCTION

It is often difficult to interpret the data of typical simple infrared (IR) sensor systems. In systems with a single IR sensor, an estimation of distance to an obstacle can be made as long as the orientation is known. A look-up-table or model of the sensor response will be required as the level is a complicated function of the emitter beam-spread, obstacle reflectivity, and detector response.

Addition of a second sensor should make it possible to determine both angle and distance. However, in typical systems orientation is usually measured as a binary: either the relative orientation is perpendicular, or it is not. Even this binary measure can be compromised if the responses of the detectors are not equivalent.

This paper describes a simple, yet effective algorithm to determine distance and orientation of a simple IR sensor array with respect to an obstacle. The assumption made here is that the obstacle is a large surface of consistent texture: a white wall, for example.

* This work was supported in part by the Natural Sciences and Engineering Research Council (NSERC) of Canada under grant OGP170446 to M. Meng.

† To whom all correspondence shall be addressed.

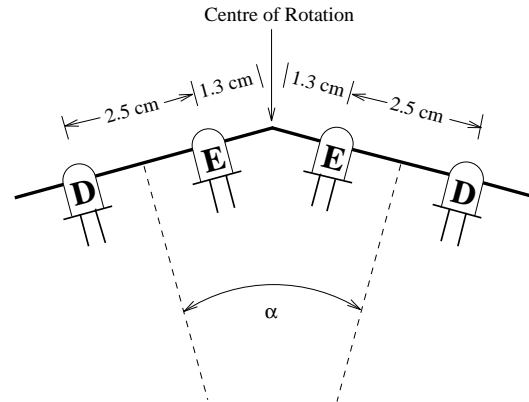


Figure 1: IR Sensor array configuration. E – IR emitter, D – IR detector. The angular separation, α , is 40° .

In addition to being effective, this algorithm is intended to be relatively simple as it is to be used in conjunction with navigation sensor data to close a navigation control loop in mobile robots with limited computational resources.

The IR sensor array configuration used throughout this paper is shown in Fig. 1. The reason for using such a physical structure is discussed later.

II. SENSOR DATA COLLECTION SYSTEM

The mechanical configuration used to gather sensor data to develop this algorithm is a simple translational-rotational two degree-of-freedom (DOF) system that uses stepping motors as the actuators. It allows gathering of sensor level data at distances in increments of 0.3 mm and angles in increments of 1.8° .

To interface the mechanical system to a PC, an MC68HC11 single-board computer (SBC) is connected through the serial port. The SBC uses eight digital output lines to control the stepping motors (via H-bridge drivers), and two analog to digital converter lines to sample the IR sensor data. Data is collected by using

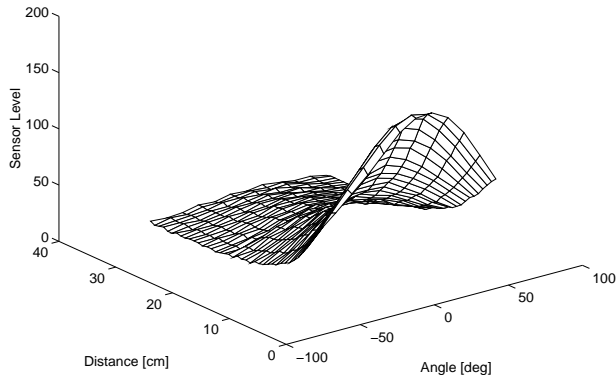


Figure 2: The response of the right sensor.

a capture feature on the PC terminal program while the HC11 runs an embedded program to step through distance and angle ranges.

Fig. 2 is a sample of the data collected for the right sensor of the array shown in Fig. 1. Some of the data points have been dropped in order to create a clearer plot. The range of distances and angles for which the sensor levels are measured is limited by the workspace of the 2 DOF manipulator.

III. SENSOR FUSION

To describe the warping algorithm successfully, it is necessary to describe the sensor fusion process. The closed-form of the algorithm automatically performs the fusion and it is easy to lose physical insight into what actions are performed.

Sensor fusion is achieved by performing a *modal-binary* transformation [1] on the sensor data. This process is a simple one: a sensory image is created by plotting the sensor levels against one another. The current state of the sensor array corresponds to a single pixel (which is either on or off) in this image. Other methods of image construction exist which may be more suitable depending upon the requirements of the target system. For instance, a modal-frequency transformation would increase a pixel's 'intensity' when the sensor levels corresponding to the pixel are encountered. Using this approach, sensor noise and uncertainty can be reduced by sampling the sensor levels repeatedly and using standard image processing algorithms, such as thresholding, to select the best response.

The modal-binary image has a strong physical meaning. Intuitively, if the two sensor responses were identical, points along a line through the origin with a slope of 1 would indicate that the sensor array is at a right angle to the object. The closer the point is to the origin

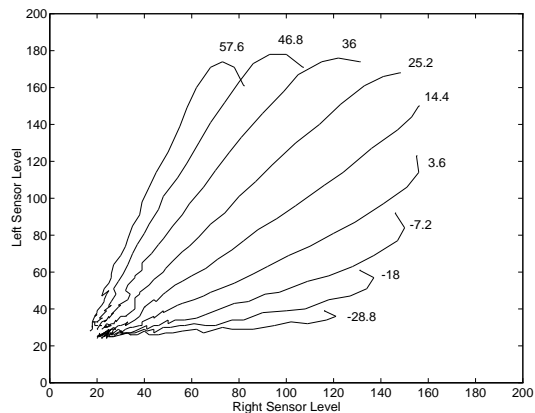


Figure 3: Constant angle curves in the modal-binary sensory image (specified in degrees).

of this image, the further it is from the obstacle.

Figs. 3 and 4 show curves of constant angle and constant distance, respectively, for the sensor configuration of Fig. 1. These curves indicate that we are not dealing with ideal (identical) devices. Normalization of the sensor data with respect to one-another prior to creation of the sensory images would yield a more ideal response, but it was decided that this is an unnecessary step for this simple algorithm; as long as the algorithm operates correctly, it is unimportant what the sensory image actually looks like.

The algorithm will work successfully only if the constant angle (and distance) curves are unique. When the curves intersect one another, no unique solution exists and the algorithm fails in this region. The greater the separation between the curves, the more accurate the algorithm will be. The separation is dictated by the nature of the response of IR sensors, and of the physical configuration of the sensor array. This is behind the selection of the array shown in Fig. 1. Without the angular separation, α , between the left and right sensors, the constant angle curves lie uncomfortably close to each other.

IV. THE WARPING ALGORITHM

The objective of the warping algorithm is to map the sensor levels into an image with distance and angle coordinates. The constant angle and distance curves presented in the last section provide insight into how the warping is to occur.

There are several distinct steps that need to be followed in order to obtain a closed form of the final mapping (warping).

1. Models of sensor level variation with respect to

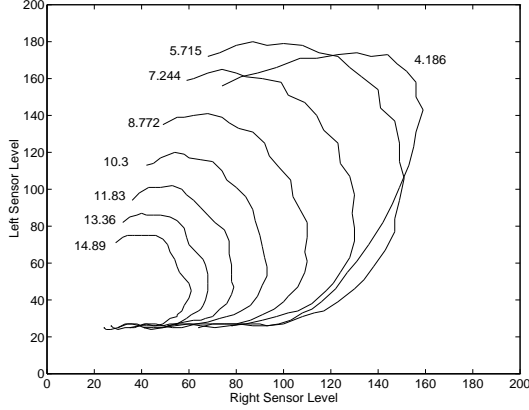


Figure 4: Constant distance curves in the modal-binary sensory image (specified in cm).

distance and angle are created.

2. Models of how distance varies with respect to sensor level and angles are derived based upon the model in (1), above.
3. The closed form of the mapping is determined by equating the two models determined in (2) and solving the resulting equation.

It was found that constructing a model of the sensor levels was necessary since the raw data from the sensors has noise. This potentially creates double-valued functions which yield poor results if directly used in modelling the distance response in (2). Viewed in this manner, constructing a model of the sensor levels serves as a noise filter.

A. Modelling Sensor Level Response

To construct a model of the sensor level, s , with respect to angle, θ , and distance, d , a 5th-order least-squares method is used¹. First, ‘slices’ of the sensor levels at constant distances are modelled for each and every distance. The 6 parameters which define the models are then themselves modelled according to the change in distance. Such a model can be expressed as:

$$s = f(d, \theta) = \Theta_{1 \times 6} \mathbf{P}_{6 \times 6} \mathbf{D}_{6 \times 1} \quad (1)$$

where

$$\Theta = [\theta^0 \quad \theta^1 \quad \theta^2 \quad \theta^3 \quad \theta^4 \quad \theta^5], \quad (2)$$

$$\mathbf{D} = [d^0 \quad d^1 \quad d^2 \quad d^3 \quad d^4 \quad d^5]^T, \quad (3)$$

¹ This stage of modelling is not used during actual implementation of the algorithm on a mobile robot; it is an intermediate stage that is performed only once in obtaining the final closed-form mapping. As a result, use of rather bulky 5th order models is not problematic.

and each row of \mathbf{P} is a 5th-order model of the angle variation parameters with respect to distance.

Both the left and right sensors are modelled in this manner. They are then used to create sensor level responses for each distance and angle of interest.

B. Modelling the Distance Relation: A ‘Contour’ Model

From the response of the models found in the last subsection, a series of level contours are formed from which ‘inverse’ models are derived. All contours corresponding to a sensor level, s , in the range of distances of interest are modelled with respect to angle, θ , using a second order polynomial. These three parameters are then individually modelled using a third order polynomial to yield an expression for distance, d . In matrix form,

$$d = g(s, \theta) = \Theta_{1 \times 3} \mathbf{M}_{3 \times 4} \mathbf{S}_{4 \times 1} \quad (4)$$

where

$$\Theta = [\theta^0 \quad \theta^1 \quad \theta^2], \quad (5)$$

$$\mathbf{S} = [s^0 \quad s^1 \quad s^2 \quad s^3]^T, \quad (6)$$

and \mathbf{M} is the matrix of model parameters. Both the left and right sensor distance responses are modelled in this manner.

Contrary to the last modelling process, the lowest possible model order was chosen here. This not only reduces the computational burden, but it also leads to a closed-form solution. In certain situations, accuracy requirements may dictate use of higher order models.

C. Obtaining a Closed-Form Warping

The closed-form of the warping is obtained by equating the distance models (Eq. 4) for the two sensors and solving the resulting quadratic:

$$\Theta (\mathbf{M}_l \mathbf{S}_l - \mathbf{M}_r \mathbf{S}_r) = 0 \quad (7)$$

where the subscript r denotes the right sensor and l denotes the left. For the sensor configuration of Fig. 1, the models were determined to be:

$$\mathbf{M}_r = \begin{bmatrix} 52.7 & 2.9 \times 10^{-2} & -4.5 \times 10^{-3} \\ -1.2 & -2.4 \times 10^{-4} & 7.1 \times 10^{-5} \\ 1.1 \times 10^{-2} & -3.4 \times 10^{-6} & -6.4 \times 10^{-7} \\ -3.4 \times 10^{-5} & 4.1 \times 10^{-8} & 1.4 \times 10^{-9} \end{bmatrix}^T \quad (8)$$

$$\mathbf{M}_l = \begin{bmatrix} 32.8 & 4.9 \times 10^{-1} & -5.5 \times 10^{-4} \\ -0.6 & -5.9 \times 10^{-3} & -8.0 \times 10^{-5} \\ 4.4 \times 10^{-3} & 5.3 \times 10^{-5} & 8.7 \times 10^{-7} \\ -1.3 \times 10^{-5} & -1.5 \times 10^{-7} & -3.0 \times 10^{-9} \end{bmatrix}^T \quad (9)$$

Solving the quadratic yields two values for the angle. The solution which falls within the modelled range is

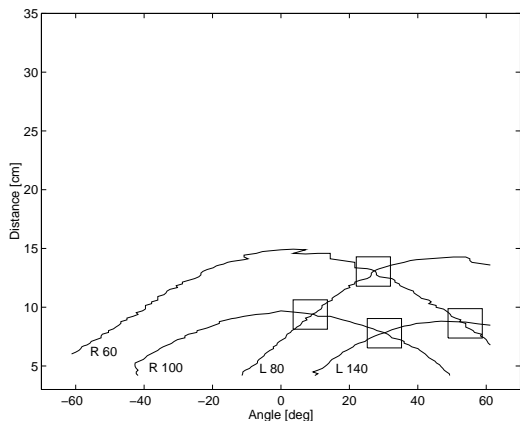


Figure 5: Graphical interpretation of the solution of the quadratic.

selected. If both solutions are candidates, the distance, calculated by placing the angle solutions into Eq. (4), is used as the deciding criterion.

Fig. 5 shows the graphical interpretation of the solution of Eq. (7). In this figure, four contours are shown in the distance-angle plain: two for the right sensor level and two for the left sensor level. The intersection points of these curves are the solutions that we are looking for.

V. RESULTS

Figs. 6 and 7 show magnitude error contours of the results determined by the closed-form warping. The errors indicate that it is necessary to limit the possible sensor level ranges by limiting the physical region in which the sensor array is to operate. The size of the operating region is dictated by the amount of error that is tolerable within the system.

To reduce the error it would be possible to increase the accuracy of the modeling process. Unfortunately this increases the computational requirements.

VI. CONCLUSIONS

This paper has successfully derived a simple method to determine the angle and distance of a dual IR sensor array relative to an obstacle based upon the sensor levels. The algorithm is found to be effective within a region whose size is influenced by the accuracy of the modelling process and the physical configuration of the sensor array. The algorithm is simple and its closed-form permits use in applications where computational resources are scarce, such as simple autonomous mobile robotics.

Future research directions on this topic include implementation of a wall-following behaviour using the sensor array and the algorithm described here. Also

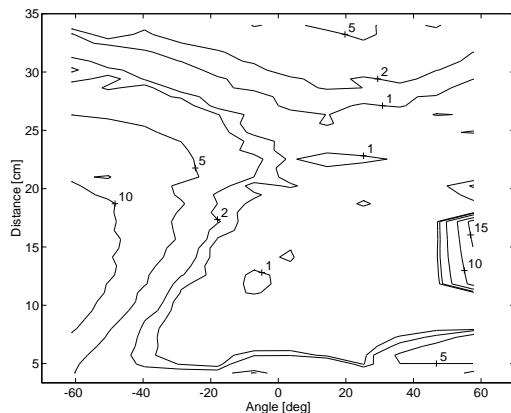


Figure 6: Distance magnitude error contours (in cm).

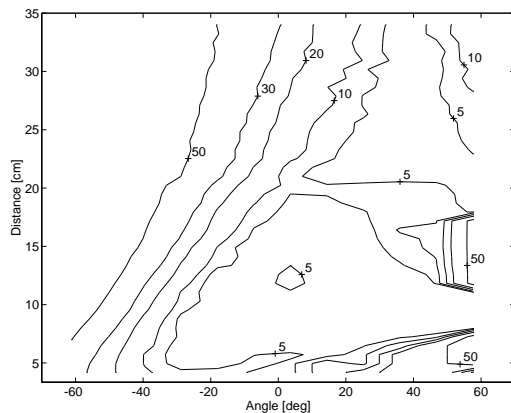


Figure 7: Angle magnitude error contours (in degrees).

planned is an expansion of the algorithm to include interpretation of information from a third sensor to determine the β -space position and orientation of the sensor system with respect to an obstacle. Additionally, incorporation of a simplified measure of an obstacle's surface texture is proposed in order to expand the algorithm's use into more general situations. A sensor array will be mounted on the end-effector of a PUMA 560 manipulator (located in the ART Lab) and control loops will be closed using the enhanced algorithm.

REFERENCES

- [1] R.M. Joseph, J.J. Rowland, and H.R. Nicholls. Image analysis of diverse sensor data. In *IEEE International Conference on Systems, Man and Cybernetics*, pages 700–705, 1994.